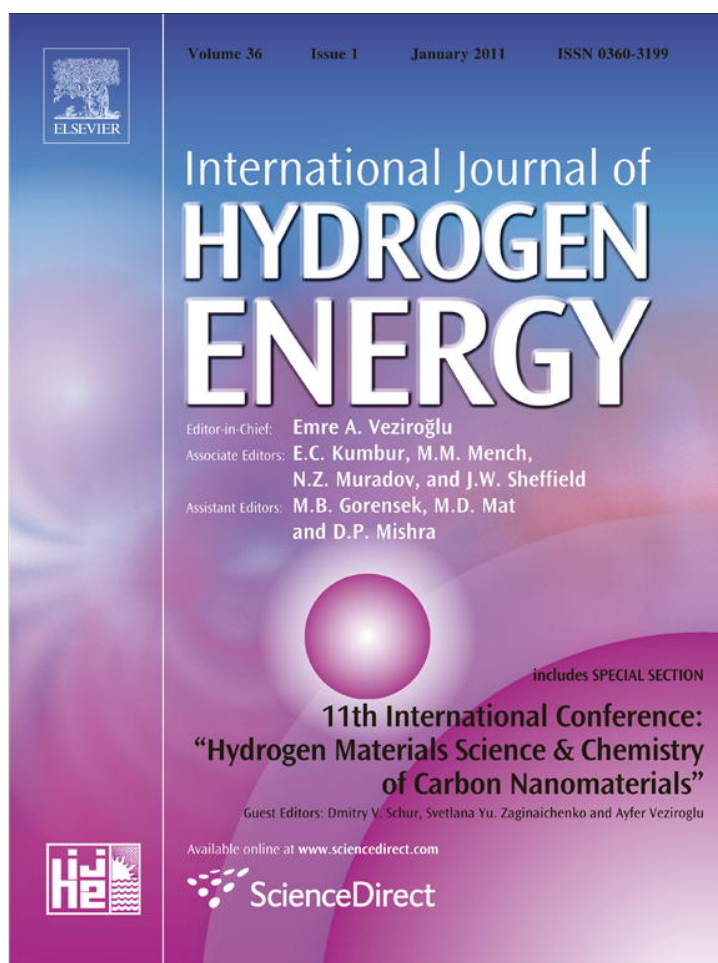


Provided for non-commercial research and education use.  
Not for reproduction, distribution or commercial use.

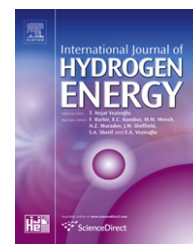


This article appeared in a journal published by Elsevier. The attached copy is furnished to the author for internal non-commercial research and education use, including for instruction at the authors institution and sharing with colleagues.

Other uses, including reproduction and distribution, or selling or licensing copies, or posting to personal, institutional or third party websites are prohibited.

In most cases authors are permitted to post their version of the article (e.g. in Word or Tex form) to their personal website or institutional repository. Authors requiring further information regarding Elsevier’s archiving and manuscript policies are encouraged to visit:

<http://www.elsevier.com/copyright>

Available at [www.sciencedirect.com](http://www.sciencedirect.com)journal homepage: [www.elsevier.com/locate/he](http://www.elsevier.com/locate/he)

# Vertical release of hydrogen in a partially enclosed compartment: Role of wind and buoyancy

Kuldeep Prasad\*, Jiann Yang

National Institute of Standards and Technology, 100 Bureau Drive, Stop 8663, Gaithersburg, MD 20899, United States

## ARTICLE INFO

### Article history:

Received 25 June 2010

Received in revised form

2 August 2010

Accepted 9 August 2010

### Keywords:

Hydrogen

Dispersion

Wind

Analytical model

## ABSTRACT

The natural and wind driven mixing and dispersion of hydrogen released in an accidental manner in a partially enclosed compartment with two vents is investigated using theoretical tools. A simple analytical model is constructed to predict the entrainment of air in a buoyant turbulent hydrogen plume and the properties of the resulting two-layer stratification that drives the flow through the vents. Air flows in through vents below the position of neutral buoyancy and exits from vents above it. CFD simulations are conducted in a full-scale geometry to confirm the physical phenomena and to compare with the analytical results. Analytical results are also compared with experimental data from a ¼ scale two-car residential garage. The analytical model is used to understand the important physical processes involved during hydrogen release as a vertical plume, and dispersion in a compartment with vents at multiple levels, with and without a steady wind. Parametric studies are conducted to study the effect of hydrogen release rate on location of the interface between the two layers and hydrogen volume fraction in the upper layer. Analytical model results indicate that for a given hydrogen release rate, the hydrogen concentration in the upper layer reaches a maximum under wind conditions that oppose the buoyancy induced flow, and that this maximum value can be as much as 70% higher than the case with no wind effects. Results also indicate that blowing outdoor air into the lower vent is an effective strategy for reducing the flammable volume of hydrogen gases in a compartment, following an accidental release.

Published by Elsevier Ltd on behalf of Professor T. Nejat Veziroglu.

## 1. Introduction

As more hydrogen fueled applications enter the marketplace, there is a need for a better understanding of the potential for fires and explosions associated with the unintended release of hydrogen within an enclosure [1]. If hydrogen gas is released accidentally in a fully enclosed space, then the risk of an explosion will be relatively small if the total volume of the hydrogen release is smaller than 4% (lower flammability limit) or greater than 74% (upper flammability limit) of the enclosure volume, under the well-mixed assumption [2,3]. If the release

occurs in an un-enclosed space, then the buoyant hydrogen gas would rise up and the risk of hydrogen accumulation will be negligibly small. However, if hydrogen gas is released accidentally in a partially enclosed space, then flammable concentration of hydrogen will depend on hydrogen release rate, volume of released gases, vent location, cross-sectional area of vents, background leaks, wind speed/wind direction and thermal effects. Time-dependent and spatially evolving concentration of hydrogen in a partially enclosed compartment with leaks whose size and location may be unknown is difficult to predict. The uncertainty in predicting the concentrations can increase

\* Corresponding author. Tel.: +1 301 975 3968.

E-mail addresses: [kuldeep.prasad@nist.gov](mailto:kuldeep.prasad@nist.gov), [kprasad@nist.gov](mailto:kprasad@nist.gov) (K. Prasad).

0360-3199/\$ – see front matter Published by Elsevier Ltd on behalf of Professor T. Nejat Veziroglu.

doi:10.1016/j.ijhydene.2010.08.040

significantly due to external forces such as wind and thermal gradients. Developing a methodology to accurately predict the flammable volume, when hydrogen is released accidentally from a fuel cell in a compartment or a vehicle parked in a residential garage, is critical to the safe use of hydrogen and for the development of appropriate safety codes and standards for hydrogen applications.

The dispersion, mixing, and combustion of hydrogen have been studied through experiments, theoretical methods and through the use of computational fluid dynamics (CFD) tools, and have been reported in various articles presented during the International Conference on Hydrogen Safety meetings [4,5]. A number of papers [6–9] have reported experimental data on release and dispersion of hydrogen or helium in partially enclosed compartments that can be used for validating the numerical models and for improving our understanding of the physical phenomena. Pitts et al. [10] presented a detailed experimental study on helium dispersion in a  $\frac{1}{4}$ -scale two-car residential garage. Time-resolved measurements at multiple locations in the compartment were performed, and results were presented as a function of gas flow rates and duration of the flow. The National Institute of Standards and Technology (NIST) Fire Dynamics Simulator (FDS) [11] has been used to simulate these reduced-scale experiments, where helium was used as a surrogate gas [12,13]. These calculations have indicated that CFD software is capable of simulating the release and mixing of hydrogen with clearly defined geometries and boundary conditions, but simple analytical models are needed for providing guidance for emergency responders and for development of appropriate codes and standard applications relevant to hydrogen safety. Theoretical models have been developed for ventilation flows in a room with a heated floor [14–19]. These models typically look at the effect of point heating (pure buoyant flows) or distributed heating of the entire floor instead of the release of a buoyant gas. Zhang et al. [20] modified the analytical models originally developed for smoke filling a compartment for the case of a hydrogen plume in a compartment. This model did not consider the effect of multiple vents or the effect of an external wind on hydrogen concentration in a compartment. Barley et al. [21] developed a simple one-dimensional model for understanding the hydrogen stratification in a compartment that is ventilated through two vents. Their model was limited to identifying the steady-state condition and did not consider the effect of an external wind flow or the effect of intermediate vents. The results described in this paper are more general as they cover the transient as well as the steady-state flows that develop in a partially enclosed compartment with a sudden hydrogen release. CFD software has been used extensively in the past to study hydrogen leakage and burning in complex geometries [3–25]. Swain et al. [3,22] developed a method to establish the requirements for venting in buildings that contain hydrogen fueled equipment.

There is a fundamental difference between the flow-fields that are established in a compartment when hydrogen gas is released in a cluttered environment (e.g. release of hydrogen under a vehicle) as opposed to the release in an un-cluttered environment. When hydrogen gas is released under a vehicle, the buoyant gas starts to mix rapidly with the surrounding air. The hydrogen–air mixture can leak into the passenger

compartment or accumulate under the hood, depending on the construction of the underside of the vehicle. Most of the hydrogen can escape from under the vehicle through the wheel wells and the perimeter of the vehicle as multiple plumes rising towards the ceiling. The mixing of hydrogen under the vehicle and its subsequent release in the form of multiple independent plumes, results in a well-mixed hydrogen–air mixture in the compartment. Turbulent mixing under an obstruction resulting in a well mixed hydrogen–air mixture in the compartment has been observed in full-scale experiments [26] as well as reduced scaled experiments [10]. Such scenarios have also been studied recently using analytical and CFD models [27]. On the other hand, when hydrogen is released in an un-cluttered environment, the flow field can be quite different. The turbulent hydrogen plume that develops above the release point entrains fluid as it rises. Once the plume reaches the top, it spreads radially outwards to form a buoyant layer separated from the air below by a density interface. As the depth of this buoyant layer increases, the interface descends towards the plume source, and hence the layer is fed with increasing buoyant fluid.

In this paper, simple analytical models are developed for studying hydrogen release and dispersion in a compartment where hydrogen is released vertically as a buoyant turbulent plume. CFD simulations are conducted to confirm the physical phenomena and to compare with the analytical model. Model results are compared with experimental data of helium released in a  $\frac{1}{4}$  scale garage model. The effect of hydrogen release rate and vent cross-sectional area on hydrogen volume fraction (mole fraction) and location of the interface in the compartment is discussed. The model is extended to study the effect of a wind that assists the buoyancy-driven flow, or a wind that opposes the buoyancy-driven flow. Results for hydrogen release and dispersion in a compartment under an assisting/opposing wind are presented and discussed.

---

## 2. Accidental hydrogen release in a ventilated compartment

Consider the case of a compartment of height  $H$ , in which hydrogen is leaking accidentally from a source. The light hydrogen gas will rise as a vertical plume, reach the ceiling, spread to the sidewalls and descend in the space between the sidewalls and the plume as shown in Fig. 1. If the compartment was sealed, then the upper part of the plume will be surrounded by fluid that is lighter than the fluid of the initial density. This will result in filling of the compartment and has been discussed extensively by Baines et al. [18] and Worster et al. [28]. If the compartment is vented through two vents, one located close to the floor and the other close to the ceiling, then the layer of buoyant fluid near the ceiling will drive a flow through the openings. This will result in an inflow through the vents located close to the floor and outflow through the vent located close to the ceiling. A layer of hydrogen–air mixture will form at the ceiling that is separated from the ambient fluid (air) by a density interface. The height of this interface above the floor is denoted as  $h_i$ . The depth of the buoyant upper layer will increase as the layer is fed with buoyant fluid through the plume, and the interface will descend and approach the plume

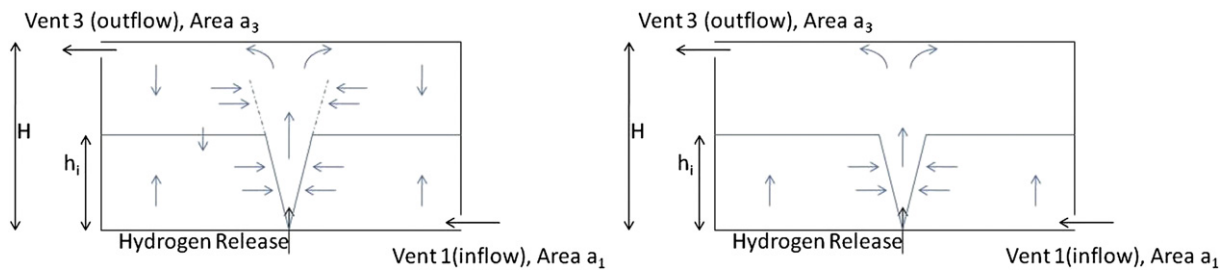


**Fig. 1 – Schematic diagram of the flow-field during the release of a light gas (hydrogen) as a buoyant turbulent plume in a compartment with vents at the top and bottom. The left sub-figure shows the flow-field during the transient stages, while the right sub-figure shows the flow-field when the interface has reached a steady state.**

source. Fig. 1 shows a schematic diagram of the flow-field during the release of hydrogen gas as a buoyant turbulent plume in a compartment with vents at the top and bottom. The left sub-figure shows the flow-field during the transient stages, while the right sub-figure shows the flow-field when the interface has reached a steady state. During the transient stages, the fluid will be rising within the plume, both above and below the interface. Outside the plume, the vertical component of velocity will be downward, decreasing to zero as the interface is approached, while below the interface the vertical component of velocity will be upward, again decreasing to zero at the interface. The horizontal component of the velocity will be towards the plume, representing the entrainment of air into the plume (Fig. 1 left sub-figure).

After some time, steady state will be achieved when the location of the interface will not change with time (Fig. 1 right sub-figure). The fluid below the interface will consist of pure ambient fluid, while above the interface the fluid will be lighter than the ambient fluid. Under steady-state conditions, the compartment will be vertically stratified with outdoor air entering through the lower vents and a lower density mixture of hydrogen and air leaving through the upper vent. The lower part of the compartment is comprised of ambient air, except in the region surrounding the hydrogen plume.

The compartment is assumed to be vented through two vents; “Vent 1” is located at the base of the compartment close to the floor, also referred to as the “lower” vent, and “Vent 3” is located at the top of the compartment, also referred to as the “upper” vent. Subscript 2 is used for intermediate vents, consistent with previous work in this subject [27]. The two

vents have cross-sectional area  $a_1$  and  $a_3$ , where suffixes 1 and 3 correspond to the respective vents. Let  $M_{H_2}$  be the mass flow rate of pure hydrogen gas into the compartment. We denote the velocity of the fluid through the lower and upper vent as  $v_1$  and  $v_3$ , respectively. It is assumed that the flow through each opening is unidirectional at any given instant in time. In general, the velocity  $v_j$  of a gas mixture through a vent  $j$  is related to the pressure drop  $\Delta P_j$  using Bernoulli’s theorem,

$$v_j = \sqrt{\frac{2\Delta P_j}{\rho}} \tag{1}$$

where,  $\rho$  corresponds to the density of the gas mixture. The volumetric flow rate  $Q_j$  through vent  $j$  of area  $a_j$  is then related to the velocity  $v_j$  according to

$$Q_j = a_j \times v_j \times c_j \tag{2}$$

where  $c_j$  is the discharge coefficient that accounts for the reduction in the area of the streamlines through the vent. The discharge coefficient is a constant lying between 0.5 for a sharp expansion at the inlet and 1.0 for a perfectly smooth expansion. It should be noted that the Bernoulli’s theorem is not strictly applicable since the flows are not dissipationless.

Fig. 2 shows the pressure distribution inside and outside the compartment at the height of the lower and upper vents. The ambient pressure at the height of the upper vent outside the compartment is represented by  $P_0$ . The pressure inside and outside the compartment varies hydrostatically with height. As a consequence, the pressure at the height of the lower vent outside the compartment will be higher due to the weight of the fluid and will equal to  $P_0 + \rho_o g H$ , where  $\rho_o$  is the density of the ambient fluid and  $g$  is the gravitational acceleration. If we let  $\Delta P_c$  be the instantaneous compartment overpressure due to the release of hydrogen gas, then the pressure inside the compartment at the height of the upper vent is represented as  $P_0 + \Delta P_c$ , while that at the height of the lower vent is represented as  $P_0 + \Delta P_c + \rho g(H - h_i) + \rho_o g h_i$ , as shown in Fig. 2. Owing to the lower density of gas mixture inside the compartment, the vertical pressure gradient is lower than the vertical pressure gradient outside the compartment. These gradients are due to the weight of the fluid. The difference between these pressure gradients leads to a buoyancy-driven flow through the vents.

The pressure difference at the level of the lower vent  $\Delta P_1$  and upper vent  $\Delta P_3$  can be written as

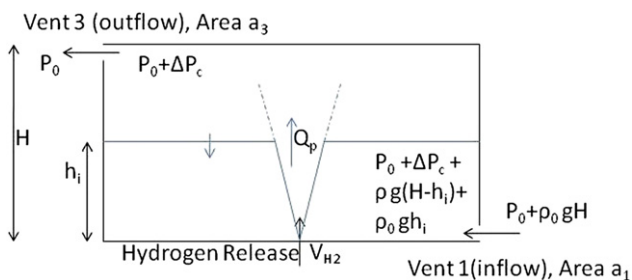


**Fig. 2 – Schematic diagram of the pressure distribution inside and outside the compartment at the height of the lower and upper vents.**

$$\Delta P_1 = \Delta \rho g(H - h_i) - \Delta P_c \quad (3)$$

$$\Delta P_3 = \Delta P_c \quad (4)$$

where,  $\Delta \rho = \rho_o - \rho$ , and  $\rho_o$  is the density of the ambient air, while  $\rho$  is the instantaneous density of the upper layer. Substituting equations for pressure difference across the vents (Equations (3) and (4)) in (1), the velocity through vent 1 and vent 3 can be expressed as

$$v_1 = \sqrt{2 \frac{\Delta \rho g(H - h_i) - \Delta P_c}{\rho_o}} \quad (5)$$

$$v_3 = \sqrt{2 \frac{\Delta P_c}{\rho}} \quad (6)$$

For any accidental release of hydrogen as a vertical plume in a ventilated compartment, it is critical to develop an accurate methodology to predict the hydrogen volume fraction in the upper layer, and the location of the interface as a function of time. Once the volume fraction and location of the interface are known, the volume of flammable gases in the compartment can be calculated. The rate of accumulation of hydrogen in the upper layer is dependent on the rate at which hydrogen gas is released in the compartment and the outflow of hydrogen through the upper vent.

$$\frac{d(\rho Y_{H_2} \times (H - h_i) \times S)}{dt} = M_{H_2} - Y_{H_2} \times \rho \times (a_3 v_3 c_3) \quad (7)$$

where,  $M_{H_2}$  is the mass flow rate of pure hydrogen gas into the compartment,  $Y_{H_2}$  is the instantaneous mass fraction of hydrogen in the upper layer and  $S$  is the cross-sectional area of the interface changes can be obtained by writing an equation for conservation of total volume (or total mass) of the upper layer. Thus

$$\frac{d((H - h_i) \times S)}{dt} = Q_p - a_3 v_3 c_3 \quad (8)$$

where,  $Q_p$  is the volumetric flow rate of hydrogen–air mixture through the plume region across the interface, discussed in more detail in sub-Section 2.1.

The ordinary differential equations (7) and (8) can be solved to obtain the instantaneous location of the interface and the density of the upper layer in a compartment, and this in turn can be used to compute the mass fraction or volume fraction of hydrogen in the upper layer as a function of time. Since the velocity (and volumetric flow rates) through the vents are related to the instantaneous compartment overpressure, an additional equation is needed to predict the instantaneous overpressure of the compartment  $\Delta P_c$ , needed to obtain the velocity  $v_3$  in equations (7) and (8). Since the volume of the compartment is fixed and assuming that the flow is incompressible, the volumetric flow rate into the compartment must equal the volume of gases leaving the compartment through the upper vent, or

$$\dot{V}_{H_2} + a_1 v_1 c_1 = a_3 v_3 c_3 \quad (9)$$

where,  $\dot{V}_{H_2}$  is the volumetric flow rate of pure hydrogen gas release into the compartment and can be obtained by dividing the mass flow rate  $M_{H_2}$  by the density of pure hydrogen gas  $\rho_{H_2}$ .

Equation (9) along with equations (7) and (8) form a system of equations that were solved to obtain the height of the interface  $h_i$ , the density  $\rho$  of the upper layer and the compartment overpressure  $\Delta P_c$  as a function of time. Equations (7) and (8) are ordinary differential equations that were advanced in time using a second order Runge Kutta (RK) method (midpoint method), followed by a Newton Raphson iteration to solve the volume conservation equation (9). The volumetric flow rates through the lower and upper vent can be obtained using equation (2) along with equations (5) and (6).

### 2.1. Plume modeling

As discussed in the previous section, equation (8) requires an expression for the volumetric flow rate  $Q_p$ , through the plume at the level of the interface. This flow rate through the plume changes due to entrainment of the surrounding air into the turbulent plume. Most laminar plumes are unstable quite close to the source, and the flow in a plume will be turbulent following a short transition region, for all but the weakest plumes [29–31]. The classical plume mixing model (Morton et al. [30]) provides a reasonable first-order estimate of the mixing, if the vertical distance from the source to the density interface far exceeds the distance required for the transition. It is assumed that the hydrogen releasing from the source is governed by the self-similar plume solution described by Morton et al. [29,30]. The plume theory predicts that the volumetric flow rate  $Q$  in the plume in an un-stratified environment varies as a function of height  $z$  measured above the release point, and can be expressed as

$$Q(z) = \frac{6\epsilon}{5} \left( \frac{9\pi^2 \epsilon}{10} \right)^{1/3} B_o^{1/3} (z + z_o)^{5/3} \quad (10)$$

where,  $\epsilon$  is the “entrainment constant” [29],  $B_o$  is the flow rate of buoyancy,  $z_o$  is the distance of the effective origin behind the source at which a pure source of buoyancy with zero volume flux and zero specified momentum flux produces an identical flow ahead of the real source [32]. The value for the entrainment constant was chosen as  $\epsilon = 0.102$  based on the most commonly used value in the literature [14–21]. The rate of flow of buoyancy  $B_o$  is related to the volumetric flow rate of hydrogen  $\dot{V}_{H_2}$  using the equation

$$B_o = \dot{V}_{H_2} \times \left( \frac{\rho_o - \rho_{H_2}}{\rho_o} \right) \times g \quad (11)$$

while,  $z_o$  can be obtained using the relation

$$\dot{V}_{H_2} = \frac{6\epsilon}{5} \left( \frac{9\pi^2 \epsilon}{10} \right)^{1/3} B_o^{1/3} z_o^{5/3} \quad (12)$$

Using this approximate model, the volumetric flow rate through the plume at a height  $h_i$  (location of the interface) can be written as

$$Q_p = \frac{6\epsilon}{5} \left( \frac{9\pi^2 \epsilon}{10} \right)^{1/3} B_o^{1/3} (h_i + z_o)^{5/3} \quad (13)$$

Equation (13) provides an additional relationship that quantifies the plume volumetric flow rate at the interface, required in Equation (8).

## 2.2. Comparison of analytical model with full scale compartment simulations

The simple analytical model discussed above was compared with results of a numerical simulation performed using the NIST Fire Dynamics Simulator (FDS). FDS is a CFD package [11] that has been used by the fire protection community to simulate fires in large buildings and for forensic analysis, and can be used effectively for modeling hydrogen release and dispersion in a compartment. The FDS software has been validated with a series of experiments that have been performed at NIST in which helium was released into a ¼-scale two-car residential garage [12,13]. Time-resolved measurements of helium volume fractions were made at multiple heights in the model garage during the release and dispersion phase [10]. FDS simulations of the experimental setup were conducted to accurately resolve the entrainment into the buoyant plume and the leakage through the vents. Simulation results indicated that FDS software can reliably predict the hydrogen release and dispersion in a compartment with specified vent locations. The results of the analytical model from the previous section are now compared with the simulations from a detailed CFD calculation (Fig. 3).

The dimensions of the compartment used for this comparative study were 6.0 m × 6.0 m × 3.0 m, with a total volume of 108 m<sup>3</sup>. Pure hydrogen gas was uniformly released through a square cross-section of 0.28 m × 0.28 m (area of 0.0784 m<sup>2</sup>). The mass flow rates of hydrogen gas were set at 5.0 kg/h, 0.5 kg/h and 0.05 kg/h, while the duration of the release was four hours. The compartment was vented through two square vents located at the top and bottom of the side-walls as shown schematically in Fig. 1. Each vent had a cross-sectional area of 0.01 m<sup>2</sup>. The computational domain was divided into eight meshes that were chosen to resolve the flow through the release chamber and the vents. Grid resolution in the computational domain was 2 cm in the horizontal and vertical direction to resolve the flow through the plume region as well as capture the transition between the upper and lower

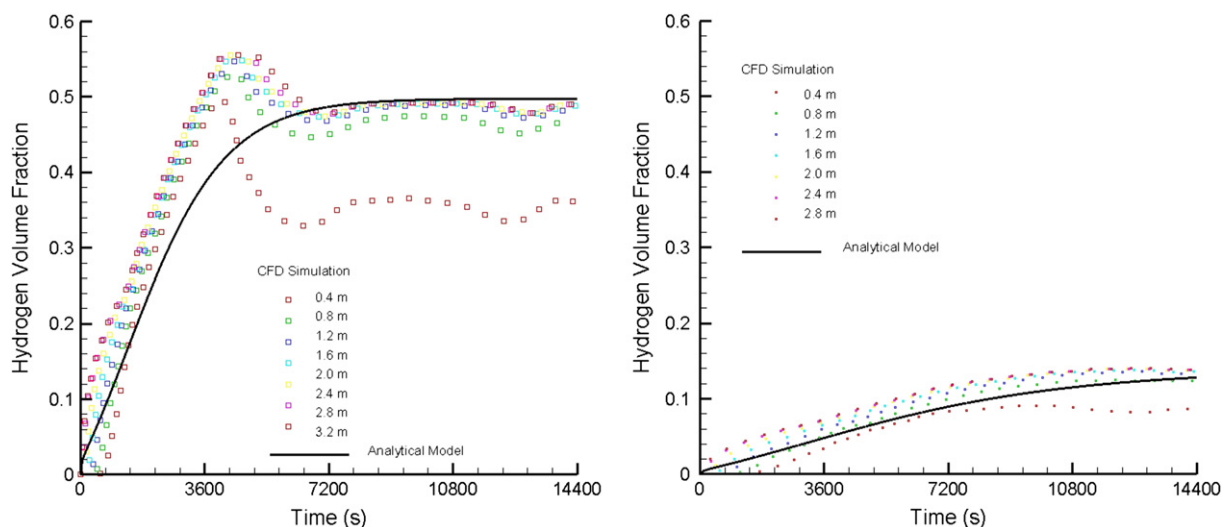
layer. Typical computational costs of a simulation performed on an eight processor machine were approximately 200 h.

Fig. 3 shows the numerically predicted hydrogen volume fraction (symbols) at seven different heights (m) in the compartment for hydrogen release rates of 5.0 kg/h (left sub-figure) and 0.5 kg/h (right sub-figure). The analytical model developed in the previous section (Fig. 3 solid line) was compared with the average value of the sensors located in the upper layer at the end of the release period. The top six sensors located close to the ceiling were used for the averaging process and the average value is representative of the properties of the upper layer. For a hydrogen release rate of 5.0 kg/h, the maximum difference between the analytical value and the average sensor value was less than 1.5%. Similarly, for a hydrogen release rate of 0.5 kg/h, the maximum difference was less than 1.0%.

## 2.3. Comparison of analytical model with reduced scale experiments

A series of experiments were conducted at NIST to characterize the dispersion of helium gas in a ¼-scale two-car residential garage [10]. In these experiments, helium (used as a surrogate for hydrogen, due to safety concerns) was released at a constant rate into a scaled model having interior dimensions of 1.5 m × 1.5 m × 0.75 m. Volumetric flow rates of helium were 3.71 L/min for four hour releases. Helium was released through a Fischer burner with a 3.6 cm diameter circular opening located 20.7 cm above the floor. Two equal square vents, with 2.15 cm sides, were placed in one of the sidewalls, with the bottom edge of the lower vent 2.54 cm above the floor and the top edge of the upper vent is located 2.54 cm below the ceiling. Helium volume fractions were recorded at seven locations along a vertical line located 37.5 cm from the left and front walls, and the relative uncertainty in the measurement was reported as 1% [10].

Fig. 4 shows the comparison of analytical model results (solid line) with experimental data (symbols). The analytical



**Fig. 3** – Comparison of analytical model results (solid line) with FDS simulations (symbols) performed in a full-scale compartment with hydrogen release rates of 5.0 kg/h (left sub-figure) and 0.5 kg/h (right sub-figure). FDS simulation results are shown for seven sensor located at various heights (m) above the floor.

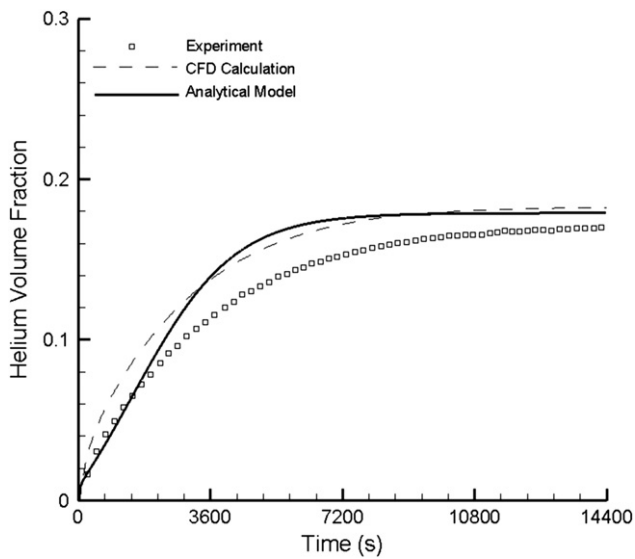


**Fig. 4 – Comparison of results of analytical model (solid line) with experimental data (symbol) from reduced scale experiments measured at a height of 65.0 cm above the floor. Results from an FDS simulation (dashed line) at the same height are also indicated.**

model results are comparable with the value measured by the sensor located at a height of 65.0 cm above the floor. Again, this sensor value is chosen since it is representative of the value in the upper layer. It is noted that since the release rate of helium employed in the experimental study are very small, diffusion of hydrogen from the upper layer into the lower layer becomes significant. The analytical model does not consider the diffusion process, and as a result over-predicts the experimental data. Fig. 4 also shows the comparison of analytical model results (solid line) with those from an FDS calculation (dashed line), measured at a height of 65.0 cm above the floor. The FDS calculations were performed for the reduced scale geometry discussed in this section. Results indicate that the analytical model results compare favorably with CFD simulations as well as experiments [10] performed in a reduced scale garage geometry.

**2.4. Effect of release rate on steady state and transient profiles**

The effect of changing the hydrogen release rate on steady state and temporally evolving hydrogen volume fraction in the upper layer, height of the interface, as well as compartment overpressure are discussed below. The geometry of the compartment is identical to that discussed in Section 2.2. Fig. 5 shows the effect of changing the hydrogen mass flow rate (release rate) from 5.0 kg/h to 0.01 kg/h on the steady-state hydrogen volume fraction, height of the interface and compartment. The profiles for these variables as a function of time for hydrogen release rates of 5.0 kg/h, 1.0 kg/h and 0.1 kg/h are shown in Fig. 6. The steady-state volumetric flow rates through the lower and upper vent are shown in Fig. 7 (left sub-figure), while the time-dependent profiles are shown in Fig. 7 (right sub-figure).

The steady-state value of the hydrogen volume fraction increases with higher hydrogen mass flow rate. The hydrogen volume fraction in the upper layer increases monotonically with time for all hydrogen release rates (rate of increase is higher for higher hydrogen mass flow rate), until a steady-state value is reached. Results indicate that the steady-state is reached faster as hydrogen release rate increases. The height of the interface (distance measured from the floor) initially reduces with time, reaches a minimum value, followed by a small increase before stabilizing at the steady-state value. The height of the interface reduces with hydrogen release rates, implying that the steady-state thickness of the upper layer increases as the hydrogen mass flow rate increases. The initial thickness of the upper layer was assumed to be 10% of the height of the compartment (chosen to approximate the thickness of the ceiling jet). Analytical model results were found to be relatively insensitive to this assumption. The compartment overpressure also increases monotonically with time initially, and then stabilizes at a value that is higher for increasing hydrogen mass flow rates.

The volumetric flow rates are shown as positive, when the flow enters the compartment and negative, when the flow leaves the compartment. For all hydrogen release rates, the steady-state value of the volumetric flow rate through the lower vent is a positive value (indicating inflow), while that through the upper vent is a negative value (indicating outflow). For a very

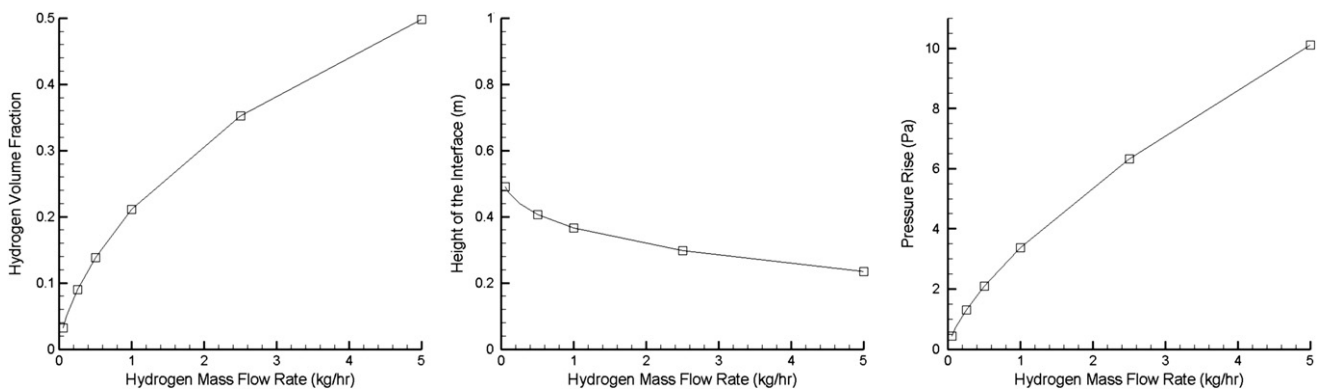


**Fig. 5 – Steady-state predictions (analytical model) on hydrogen volume fraction (left sub-figure), height of the interface (middle) and compartment (right sub-figure) plotted as a function of hydrogen mass flow rates.**

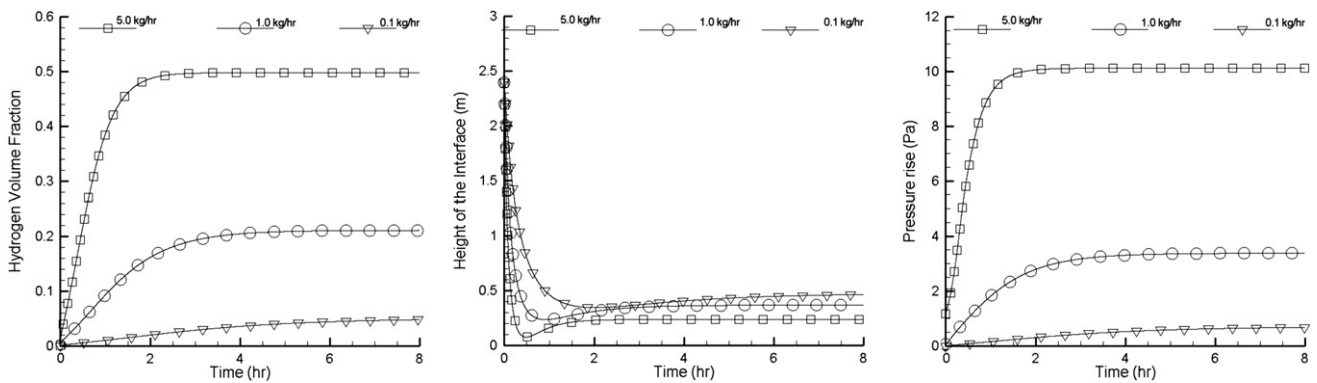


**Fig. 6 – Hydrogen volume fraction, height of the neutral layer and compartment plotted as a function of time for hydrogen release rates of 5.0 kg/h, 1.0 kg/h and 0.1 kg/h.**

short duration immediately following the release of hydrogen, the transient volumetric flow rates through the upper and lower vents are negative numbers indicating that the flow is out of the compartment through both the vents. The magnitude of the outflow through the lower vent is larger for larger hydrogen release rates. Gradually, the volumetric flow rate through the lower vent becomes a positive number indicating that outdoor air is entering the compartment through the lower vent. Results indicate that as the hydrogen release rate increases, it takes longer for the flow through the lower vent to change direction. At each instant in time, the volumetric flow rates are such that they balance the hydrogen release rate to satisfy volume conservation. The steady-state values of the volumetric flow rates (magnitude) through the lower and upper vents increase with increasing hydrogen mass flow rates. The steady-state condition also indicates inflow through the lower vent and outflow through the upper vent. Under steady-state conditions, the flux through the plume at the interface equals the volumetric flow rate through the upper vent. Also, the hydrogen release rate (volumetric flow rate) is equal to the volumetric flow rate of hydrogen through the upper vent.

### 3. Effect of wind on hydrogen release in a compartment

The results in the previous section indicate that the analytical model provides reasonable predictions of the two-layer stratification that can develop during accidental release of hydrogen as a vertical plume. The stratification of the compartment induces an inflow through the lower vent and an outflow through the upper vent. In this section, we extend the analysis to consider the effect of an external wind on the ventilation of a compartment which contains a localized source of buoyant gases.

Characterizing the effect of ventilation on hydrogen release and dispersion can be accomplished through wind tunnel testing, however such tests can be time consuming and expensive to perform. CFD modeling of the effect of an external wind can be conducted, but such computations are very expensive because of the increase in the size of the computational domain to minimize the effect of boundary conditions on the ventilation. Preliminary simulations performed using

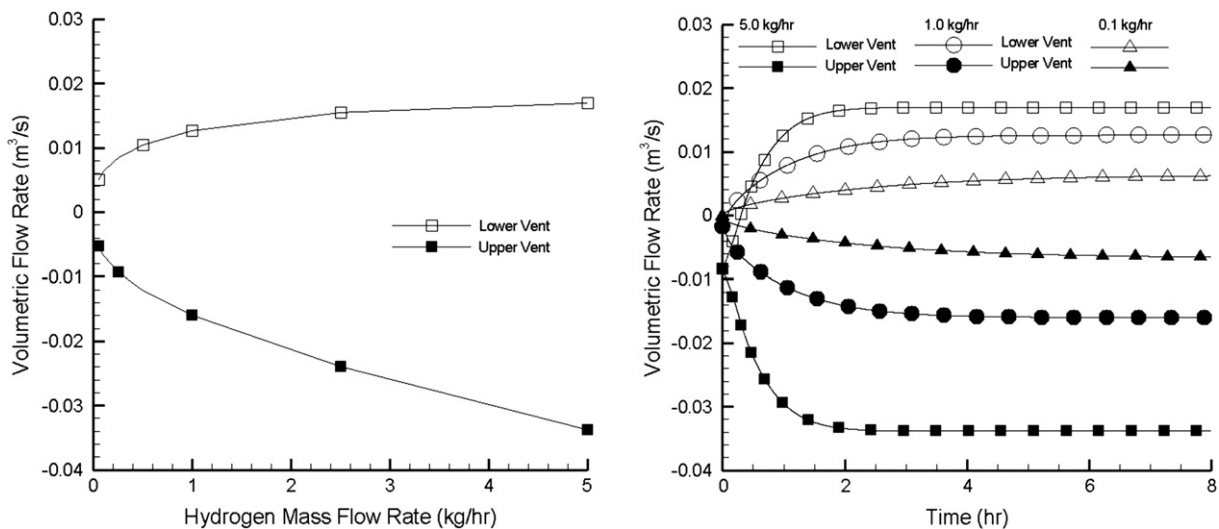


**Fig. 7 – Steady-state volumetric flow rates plotted as a function of hydrogen release rate (left sub-figure) and time dependent volumetric flow rates through the lower and upper vents for hydrogen release rates of 5.0 kg/h, 1.0 kg/h and 0.1 kg/h (right sub-figure).**

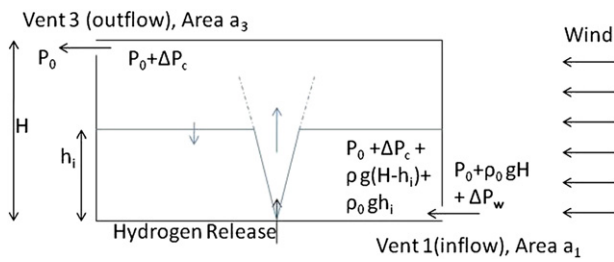


**Fig. 8 – Schematic diagram of the pressure distribution inside and outside the compartment at the height of the lower and upper vents, when a wind assists the buoyancy induced flow.**

FDS resulted in a 1700% increase in the volume of the domain, resulting in simulations that can be computationally prohibitive. Analyzing the ventilation due to an external wind using experimental or computational methods can be challenging due to the presence of fluctuations or perturbation in wind velocity and the change in direction of the wind over the duration of the release. We limit the scope of the simple models presented in this paper to situations where the wind is steady (constant speed and direction) over the duration of the release of hydrogen in the compartment. Moreover, if the hydrogen plume is subjected to an external wind flow over its entire height, then the plume may not stay vertical and may be blown over (bend away from the wind) which will violate the plume model assumptions discussed in Section 2.1. In this paper, we limit our analysis to conditions where the plume does not get blown over by the external wind. Such conditions will be obtained when the vent cross-sectional area is much smaller than the cross-sectional area of the compartment wall and the plume is located in the center of the compartment.

If the wind flow is in a direction such that it drives outdoor air into the compartment through the lower vent, then that wind assists the buoyancy induced flow. On the other hand, if the wind flow is in a direction that drives outdoor air through the upper vent into the compartment, then that wind flow opposes the buoyancy induced flow in the compartment. The effect of an external wind can be divided into two broad categories. Wind flow that assists the buoyancy induced flow are referred to as “assisting wind case”, while wind flow that opposes the buoyancy induced flow will be referred to as “opposing wind case”.

### 3.1. Assisting wind case

Wind subjects the fluid inside the enclosure to an additional driving force associated with the dynamic pressure drop between the windward and leeward openings. When the windward opening is at low level and the leeward opening is at high level, the wind assists the buoyancy-driven flow. Let  $\Delta P_w$  represent the dynamic pressure drop between the windward and leeward openings associated with the wind. This dynamic wind pressure can be related to the wind speed using Bernoulli equation  $\Delta P_w = \frac{1}{2}\rho_0 v^2$ . Fig. 8 shows the pressure distributions at the lower and upper vents, inside and outside the compartment due to the presence of an assisting wind flow. The pressure on the windward side at the lower vent is

higher due to the dynamic wind pressure  $\Delta P_w$  as shown in Fig. 8 as opposed to the case for no wind effect, shown in Fig. 2. The modified velocities through Vent 1 and Vent 3, accounting for the increased pressure due to an assisting wind, can be written as

$$v_1 = \sqrt{\frac{2\Delta\rho g(H-h_i) + \Delta P_w - \Delta P_c}{\rho_0}} \quad (14)$$

$$v_3 = \sqrt{\frac{2\Delta P_c}{\rho}}$$

For the purpose of analysis it is assumed that the flow maintains the same basic two-layer structure, observed for a wide range of wind speeds and buoyancy fluxes. The increased flow through the enclosure driven by the wind causes the interface to rise to a new level where the volume flux in the plume is equal to the volume flux produced by the wind and the buoyancy. Results for the wind assisted cases will be discussed in the Section 3.3 and contrasted with those from the wind opposed case.

### 3.2. Opposing wind case

The effect of an opposing wind on the stratification and flow produced by a rising plume in a ventilated enclosure can be much more complex than that of an assisting wind. Ventilation openings located at high level on the windward side of the enclosure and at low level on the leeward side allow a wind-driven flow from high to low level, opposite to the buoyancy-driven flow. The opposing wind case can be further divided into two categories, as discussed below.

If the wind speed that opposes the buoyancy induced flow is small (small values of wind dynamic pressure), the buoyancy-driven flow can overcome the wind driven flow. This case will result in a steady, two-layer stratification. Under

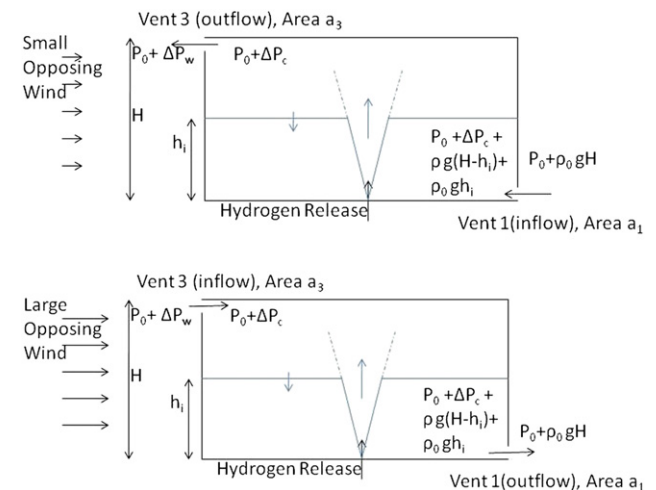


**Fig. 9 – Schematic diagram of the pressure distribution inside and outside the compartment at the height of the lower and upper vents, when a wind opposes the buoyancy induced flow. The top sub-figure shows the effect of small opposing wind, while the bottom sub-figure shows the reversal in vent flow due to a large opposing wind.**

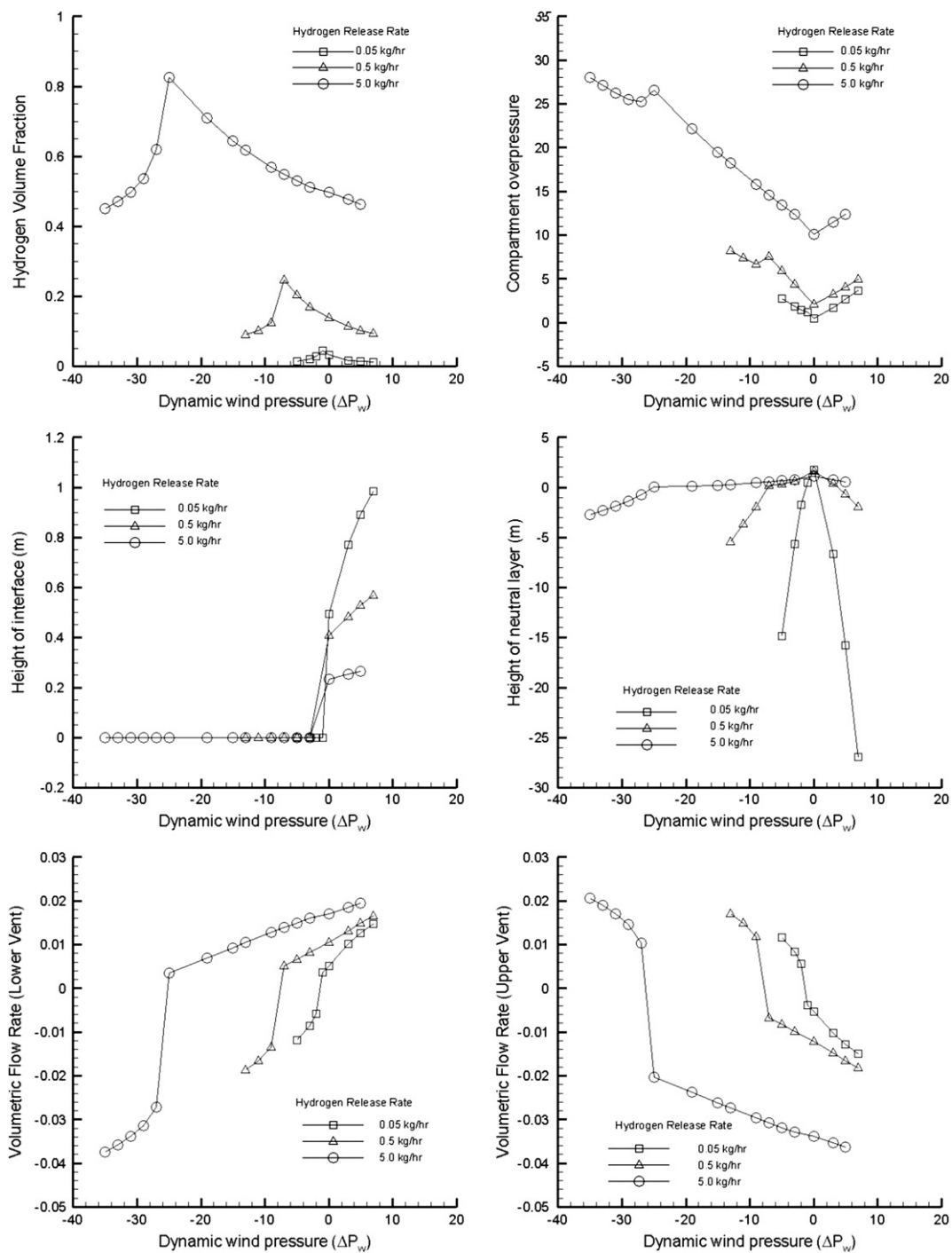


**Fig. 10 – Effect of wind overpressures on steady-state hydrogen volume fraction, compartment, location of the interface and the neutral layer, and volumetric flow rates through the lower and upper vents. Results for hydrogen release rate of 5.0, 0.5 and 0.05 kg/h have been shown.**

steady-state conditions, inflow will occur through the lower vent and outflow will occur through the upper vent. This case is shown schematically in Fig. 9 (top figure). Note, that the flow through the upper vent is outwards, indicating that the buoyancy induced flow can overcome the wind generated flow. Since the dynamic pressure on the windward side is higher by  $\Delta P_w$  for the opposed wind case as compared with no wind case, the vent velocities can be expressed as

$$v_1 = \sqrt{\frac{2 \Delta \rho g (H - h_i) - \Delta P_c}{\rho_o}} \tag{15}$$

$$v_3 = \sqrt{\frac{2(\Delta P_c - \Delta P_w)}{\rho}}$$

As the wind speed increases, the opposing wind may cause a reversal in the flow direction. In this case, ambient air enters

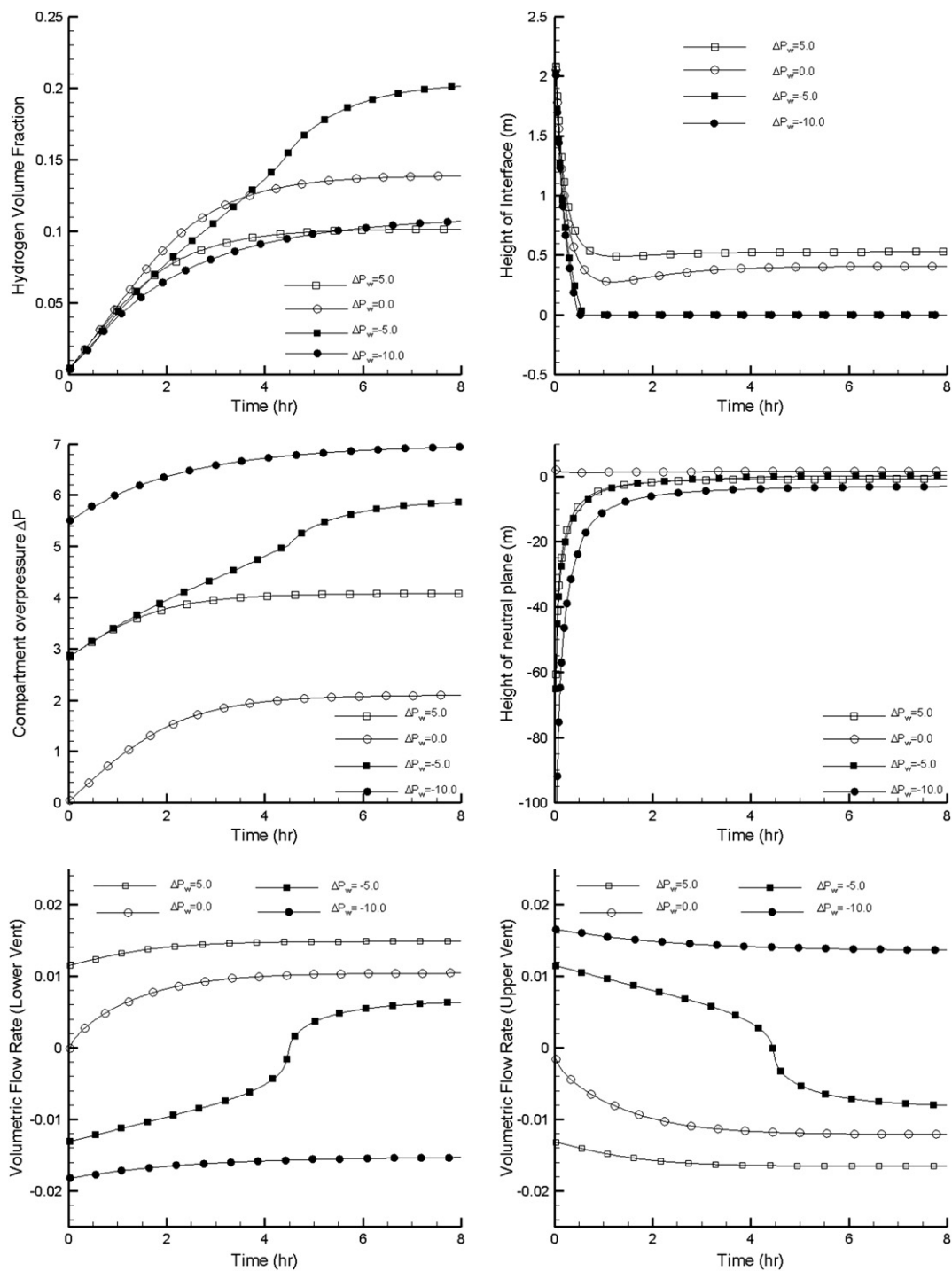


**Fig. 11 – Time dependent profiles of hydrogen volume fraction, compartment, location of the interface and the neutral layer, and volumetric flow rates through the lower and upper vents for various wind overpressures have been shown. The hydrogen release rate was set at 0.5 kg/h.**

through the high windward openings and mixes with the interior fluid, which exits through the leeward openings. If the rate of flow of hydrogen is more than the rate at which hydrogen leaves through the lower vent (leeward opening), then the buoyancy in the compartment will gradually increase and a condition will be reached where the buoyancy induced flow can overcome the wind induced flow. On the other hand,

if the flow rate of hydrogen is less than the rate at which hydrogen leaves through the lower vent (high wind speed), then the hydrogen concentration in the compartment reduces. In this situation, the stratification is destroyed and mixing ventilation occurs. Further increase in wind speed, increases the ventilation and reduces the hydrogen volume fraction in the compartment. Fig. 9 (bottom figure) shows the

pressure distributions at the lower and upper vents, inside and outside the compartment due to the presence of a high opposing wind flow. The velocities through Vent 1 and Vent 3 can now be expressed as follows, accounting for the reversal in flow direction.

$$\begin{aligned} v_1 &= \sqrt{2 \frac{-\Delta\rho g(H - h_i) + \Delta P_c}{\rho}} \\ v_3 &= \sqrt{2 \frac{(-\Delta P_c + \Delta P_w)}{\rho_o}} \end{aligned} \quad (16)$$

### 3.3. Results and discussion

Results for forced ventilation of a compartment due to an assisting and opposing wind flow are discussed in this section. The steady-state values of hydrogen volume fraction, compartment overpressure and volumetric flow rates through the lower and upper vent are shown in Fig. 10 as a function of wind overpressure  $\Delta P_w$  for various hydrogen release rates. The wind overpressure is represented as a positive value, if it is an assisting wind case; negative value, if the wind is an opposing wind, and zero, if there is no wind. Time-dependent profiles for hydrogen volume fraction in the upper layer, height of the interface, compartment overpressure and location of the neutral plane as well as volumetric flow rates through the lower and upper vent are shown in Fig. 11 for wind pressures of 5.0 Pa (assisting wind case), 0.0 Pa (no wind case) and -5.0 Pa and -10.1 Pa (opposing wind case). The hydrogen release rate was set at 0.5 kg/h.

For the assisting wind case (positive values of dynamic wind pressure or wind overpressure), the steady-state value of hydrogen volume fraction reduces and the height of the interface increases (depth of the upper layer reduces) as the dynamic wind pressure increases, for all hydrogen release rates. When the wind assists the buoyancy induced ventilation, the effect of the wind is to push the interface up until it reaches a point where the volumetric flow rates through the vents balances the flow rate of hydrogen released in the compartment. Increasing the dynamic wind pressure also results in larger steady-state compartment, which results in larger volumetric flow rates through the lower vent as well as the upper vent. The volumetric flow rates are positive for the lower vent (inflow) and negative for the upper vent (outflow) for all assisting wind cases and hydrogen release rates. The magnitude of the volumetric flow rates through the lower and upper vent increases, as the dynamic wind pressure increases. Higher volumetric inflow of outdoor air through the lower vent and larger rate of outflow of hydrogen–air mixture through the upper vent results in displacement ventilation of the compartment. The height of the interface increases and steady-state values are obtained where the hydrogen release rate balances the volumetric flow rates through the vents. Larger flow rates through the upper vent also result in lower hydrogen volume fraction in the upper layer. When the dynamic wind pressure is zero (no wind case), the compartment overpressure reaches a minimum value for each hydrogen release rate (Fig. 10).

For negative values of dynamic wind pressure (opposing wind case), the hydrogen volume fraction initially increases, reaches a maximum value, and then decreases as the

magnitude of the wind pressure increases. The maximum value of hydrogen volume fraction in the compartment is a function of the hydrogen release rate as well as the intensity of the opposing wind. The steady-state hydrogen volume fraction increases from a value of 0.49 for the no wind case, to 0.82 at a dynamic wind pressure of -25.0 Pa (negative value indicating opposing wind case) for hydrogen release rate of 5.0 kg/h. Similarly, the steady-state hydrogen volume fraction increases from 0.14 for the no wind case, to 0.25 at a dynamic wind pressure of -7.0 Pa for hydrogen release rate of 0.5 kg/h. Finally, the steady-state hydrogen volume fraction increases from 0.032 for the no wind case, to 0.044 at a dynamic wind pressure of -1.0 Pa for hydrogen release rate of 0.05 kg/h. The maximum value of steady-state hydrogen volume fraction is obtained at increasingly higher wind pressures as the hydrogen release rate increases from 0.05 kg/h to 5.0 kg/h. This maximum value of hydrogen volume fraction obtained under certain wind conditions is extremely important from a design – safety point of view, since it represents the worst case scenario. The maximum value of hydrogen volume fraction can be as much as 70% higher than its value under no wind conditions. This analysis, therefore, suggests that there is a critical dynamic wind pressure at which the compartment will reach a maximum hydrogen concentration. It is therefore important to consider the critical dynamic wind pressure condition for any compartment ventilation design/safety scenario.

For negative values of dynamic wind pressure (opposing wind case), the compartment overpressure increases and reaches a local maximum at the critical dynamic wind pressure for each hydrogen release rate. The steady-state volumetric flow rates through the lower and upper vent changes sign (change in flow direction) at the critical dynamic wind pressure. As the dynamic wind pressure increases (opposing wind case), the steady-state volumetric flow rate through the lower and upper vent reduce in magnitude from their respective values at the no wind condition. This reduction in volumetric flow rate (reduced ventilation) results in higher concentration of hydrogen in the compartment. This process continues until the critical dynamic wind pressure condition is reached. When the critical pressure is reached, the steady-state volumetric flow rates changes direction (change in sign). The volumetric flow rate through the lower vent becomes negative at this point, indicating outflow through the lower vent. At the same time, the volumetric flow rate through the upper vent becomes positive, indicating inflow through the upper vent. Thus, the maximum concentration in the compartment is reached when the flow through the vents reverses direction due to an opposed wind flow.

## 4. Conclusions and recommendations for future work

The natural and wind driven mixing and dispersion of hydrogen released in an accidental manner in a partially enclosed compartment with two vents are investigated using theoretical tools. A simple model is constructed to predict the entrainment of air in a buoyant turbulent hydrogen plume and the resulting two-layer stratification that drives the flow through the vents. The buoyancy-driven flow induces an inflow through the lower

vent and outflow through the upper vent. The analysis is based on determining the compartment overpressure and conservation equations are formulated for obtaining the time dependent hydrogen volume fraction and the interface location. Analytical model results were found to compare favorably with CFD simulations conducted in a full-scale geometry as well as with experiments performed in a quarter scale two-car residential garage. The model is extended to consider the effect of a steady external wind that either assists or opposes the buoyancy induced flow through the vents.

The effect of hydrogen release rate on hydrogen volume fraction in the compartment is presented. Steady state hydrogen volume fraction in the compartment is lower when the hydrogen release rate is smaller and the vent cross-sectional area is larger. The hydrogen volume fraction in the upper layer and the compartment overpressure monotonically increases to its steady-state value for all hydrogen release rates. However, the location of the interface does not monotonically approach its steady-state value and this effect is attributed to the change in the flow direction at the lower vent, especially at large values of hydrogen release rate. When buoyancy-driven ventilation in a compartment is assisted by a steady wind, the hydrogen volume fraction was found to reduce for all hydrogen release rates. Results indicate that the best method for reducing concentration in a compartment is to blow air into the lower vent. When the wind opposes the buoyancy induced flow, then the hydrogen volume fraction in the compartment increases and the flow through the vents reduces. The maximum hydrogen volume fraction in the compartment is reached when the flow through the vents reverses direction due to an opposed wind flow. The maximum volume fraction was found to be approximately 70% higher than the no-wind case.

The analysis has been limited to conditions in which the compartment is vented through two vents, one located close to the floor and other located close to the ceiling. Future work will focus on conditions in which multiple vents may be located at different heights in the compartment (representative of natural ventilation in a realistic garage). The effect of distance between the vents and vent cross-sectional area on hydrogen volume fraction should also be studied. The effect of an assisting or opposing wind flow on a compartment with multiple vents at various heights is critical for understanding the flow-field in realistic geometries. The effect of temperature difference between the compartment and the surroundings should also be considered to account for accidental hydrogen release in a cold climate, and to study its effect on natural ventilation. Finally, the analysis should be extended to the study of forced ventilation that is controlled by the output of a hydrogen sensor (different from wind driven ventilation) to identify effective mitigation strategies in realistic geometries.

#### REFERENCES

- [1] Leon A. Hydrogen technology. Springer; 2008.
- [2] Kuo KK. Principles of combustion. John Wiley and Sons; 1986.
- [3] Swain MR, Grilliot ES, Swain MN. Advances in hydrogen energy. New York: Kluwer Academic Publishers, Plenum Press, Dordrecht; 2000.
- [4] Proceedings of the 2nd International Conference on Hydrogen Safety, September 2007.
- [5] Proceedings of the 3rd International Conference on Hydrogen Safety, September 2009.
- [6] Tchouvelev AV, DeVaal J, Cheng Z, Corfu R, Rozek R, Lee C. Modeling of hydrogen dispersion experiments for SAE J2578 test method development. In: Proceedings of the second international conference on hydrogen safety; 2007.
- [7] Ishimoto Y, Merilo E, Groethe M, Chiba S, Iwabuchi H, Sakata K. Study of hydrogen diffusion and deflagration in a closed system. In: Proceedings of the second international conference on hydrogen safety; 2007.
- [8] Lacombe JM, Dagba Y, Jamois D, Perrette L, Proust Ch. Large-scale hydrogen release in an isothermal confined area. In: Proceedings of the second international conference on hydrogen safety; 2007.
- [9] Middha P, Hansen OR, Storvik IE. Validation of CFD-model for hydrogen dispersion. *J Loss Prev Process Ind* 2009;22: 1034–8.
- [10] Pitts WM, Prasad K, Yang JC, Fernandez MG. Experimental characteristics and modeling of helium dispersion in a ¼-Scale two-car residential garage. In: Proceedings of the third international conference on hydrogen safety; 2009.
- [11] McGrattan K, Hostikka S, Floyd J, Baum H, Rehm R, McDermott R. Fire dynamics simulator (version 5) technical reference guide. Special Publication 1018–5. Gaithersburg, MD: National Institute of Standards and Technology; 2007.
- [12] Prasad K, Bryner N, Bundy M, Cleary T, Hamins A, Marsh N, et al. Numerical simulation of hydrogen leakage and mixing in large confined spaces. In: Proceedings of the NHA annual hydrogen conference; 2008.
- [13] Prasad K, Pitts W, Yang J. A numerical study of hydrogen or helium release and mixing in partially confined space. In: Proceedings of the NHA annual hydrogen conference; 2009.
- [14] Linden PF, Lane-Serff GF, Smeed DA. Emptying filling boxes: the fluid mechanics of natural ventilation. *J Fluid Mech* 1990; 212:309–35.
- [15] Kaye NB, Hunt GR. Time-dependent flows in an emptying filling box. *J Fluid Mech* 2004;520:135–56.
- [16] Lishman B, Woods AW. The control of naturally ventilated buildings subject to wind and buoyancy. *J Fluid Mech* 2006; 557:451–71.
- [17] Batchelor GK. An introduction of fluid dynamics. Cambridge University Press; 1967.
- [18] Baines WD, Turner JS. Turbulent buoyant convection from a source in a confined region. *J Fluid Mech* 1969;37:51–80.
- [19] Gladstone C, Woods AW. On buoyancy-driven natural ventilation of a room with a heated floor. *J Fluid Mech* 2001;441: 293–314.
- [20] Zhang J, Hagen M, Bakirtzis D, Delichatsios MA, Venetsanos AG. Numerical studies of dispersion and flammable volume of hydrogen in enclosures. In: Proceedings of 2nd international conference on hydrogen safety; 2007.
- [21] Barley D, Gawlik K. Buoyancy-driven ventilation of hydrogen from buildings: laboratory test and model validation. *Int J Hydrogen Energy* 2009;34:5592–603.
- [22] Swain MR, Filoso P, Grilliot ES, Swain MN. Hydrogen leakage into simple geometric enclosures. *Int J Hydrogen Energy* 2003;28:229–48.
- [23] Swain MR, Shriber J, Swain MN. Comparison of hydrogen, natural gas, liquified petroleum gas, and gasoline leakage in a residential garage. *Energy and Fuels* 1998;12:83–9.
- [24] Vudumu SK, Koylu UO. Detailed simulations of the transient hydrogen mixing, leakage and flammability in simple geometries. *Int J Hydrogen Energy* 2009;34:2824–33.

- 
- [25] Venetsanos AG, Papanikolaou E, Delichatsios M, Garcia J, Hansen OR, Heitsh M, et al. An inter-comparison exercise on the capabilities of CFD models to predict the short and long term distribution and mixing of hydrogen in a garage. *Int J Hydrogen Energy* 2009;32(13):2235–45.
- [26] Blais M, Joyce A. Hydrogen release and combustion measurements in a full scale garage. NIST GCR 10–929; 2010.
- [27] Prasad K, Pitts W, Yang J. Effect of wind and buoyancy on hydrogen release and dispersion in a compartment with vents at multiple levels. *Int J Hydrogen Energy* 2010;35:9218–31.
- [28] Worster MG, Huppert HE. Time dependent profiles in a filling box. *J Fluid Mech* 1983;132:457–66.
- [29] Morton BR, Taylor GI, Turner JS. Turbulent gravitational convection from maintained and instantaneous source. *Proc R Soc Lond A* 1956;234:1–23.
- [30] Morton BR. Forced plumes. *J Fluid Mech* 1959;5:151–63.
- [31] Morton BR, Middleton J. Scale diagrams for forced plumes. *J Fluid Mech* 1973;58:165–76.
- [32] Hunt GR, Kaye NG. Virtual origin correction for lazy turbulent plumes. *J Fluid Mech* 2001;435:377–96.